ISSN 0023-1584, Kinetics and Catalysis, 2010, Vol. 51, No. 1, pp. 119–125. © Pleiades Publishing, Ltd., 2010.
Original Russian Text © D.I. Potemkin, P.V. Snytnikov, V.P. Pakharukova, G.L. Semin, E.M. Moroz, V.A. Sobyanin, 2010, published in Kinetika i Kataliz, 2010, Vol. 51, No. 1, pp. 129–135.

CONFERENCE

Copper–Cerium Oxide Catalysts Prepared by the Pechini Method for CO Removal from Hydrogen-Containing Mixtures

D. I. Potemkin[a,b], P. V. Snytnikov[a,b], V. P. Pakharukova[a,b], G. L. Semin[a], E. M. Moroz[a], and V. A. Sobyanin[a,b]

[a] *Boreskov Institute of Catalysis, Siberian Branch, Russian Academy of Sciences, Novosibirsk, 630090 Russia*
[b] *Novosibirsk State University, Novosibirsk, 630090 Russia*
e-mail: pvsnyt@catalysis.ru

Received October 13, 2008

Abstract—A series of copper–cerium oxide catalysts was prepared by the Pechini method, and their physicochemical and catalytic properties in CO oxidation in hydrogen-containing gas mixtures were studied. The method chosen for catalyst preparation yields finely dispersed copper and cerium oxides in the catalyst.

DOI: 10.1134/S0023158410010192

Great attention is currently given to copper–cerium oxide catalysts for CO oxidation in hydrogen-containing mixtures. The influence of the preparation method and the copper content of the catalyst on the catalytic properties was studied in many works. The catalysts were prepared by coprecipitation [1–9], deposition–precipitation [10], impregnation [7, 11–17], the sol–gel method [6, 18–20], the decomposition of a mixture of copper and cerium nitrates in the presence of urea [7, 21, 22], the chelate method [8, 23], and treatment of a mixed solution of copper and cerium salts with citric acid under standard conditions [8, 24, 25] and under hydrothermal conditions [7, 25]. Systematization of the available data suggests that the systems containing 10–25 at % Cu, or, approximately, 2–6 wt % Cu, have the best catalytic properties. Most researchers believe that copper in these systems is mainly in the dispersed state and exists as clusters on the support surface, ensuring high activity and selectivity of the catalyst. The introduction of a larger amount of copper results in the agglomeration of particles and in the appearance of large copper oxide particles (several tens of nanometers in size), which undergo reduction to copper metal in the reaction mixture.

The polymer precursor (Pechini) method is among the ways of obtaining catalysts with a high degree of dispersion and uniform component distribution. This method was initially intended for the synthesis of oxide ceramics for electronic applications [26], but later it found wide use in the syntheses of ceramic and catalytic materials [27–33]. We showed earlier [34] that the copper–cerium oxide catalysts prepared using this method are finer than the samples obtained by other methods, for instance, coprecipitation and impregnation [11, 12].

In the present work, we synthesized a series of copper–cerium oxide catalysts by the polymer precursor method, studied their catalytic properties in CO oxidation in hydrogen-containing mixtures, and characterized the state of individual components of the system by X-ray diffraction.

EXPERIMENTAL

Preparation of Catalysts

Catalysts were synthesized using a widespread Pechini technique. Copper and cerium nitrates were dissolved in water, citric acid was added to the solution ((Cu + Ce)/citric acid = 1 : 1 mol/mol), and the resulting mixture was stirred until the dissolution of the acid. Next, the solution was heated to 60°C and ethylene glycol was added dropwise under stirring (ethylene glycol/citric acid = 2 : 1 mol/mol). The solution was stirred for 2 h at ~75°C and was then left to stand at room temperature without stirring for 1 day. Next, the solution was heated again to ~85°C and was concentrated by evaporation under continuous stirring until a solidifying homogeneous mass was formed. After cooling, the mass was pounded, placed into a muffle furnace, heated at a rate of 1 K/min from room temperature to 280°C, and calcined for 6 h. Then the temperature was increased at a rate of 1 K/min to 400°C and maintained at this level for 2 h. Cerium oxide and samples with calculated copper contents of 1, 5, 10, 15, and 20 wt %, hereafter designated CeO_2, 1Cu-CeO_2, 5Cu-CeO_2, 10Cu-CeO_2, 15Cu-CeO_2, and 20Cu-CeO_2, respectively, were thus prepared.

The catalyst powders were pressed into pellets, which were then crushed. The 0.25–0.5 mm size fraction was used in catalytic experiments.

Investigation Methods

The main components in the copper–cerium catalysts were quantified by ICP-AES using an Optima instrument.

Specific surface areas (S_{BET}) were derived from complete low-temperature nitrogen adsorption isotherms (BET method) using an ASAP-2400 instrument.

X-ray diffraction patterns were obtained on an HZG-4C diffractometer (CuK_α radiation, λ = 1.5418 Å, graphite monochromator, $2\theta = 20°–120°$, 0.05° increments, counting time of 10 s per point). Qualitative phase analysis was carried out using the JCPDS database [35]. The size (D) of the coherent scattering region (CSR) and lattice microdistortion ($\Delta d/d$) were calculated from the broadening of diffraction peaks of detected phases. The peak broadening effect due to the small particle size and the same effect due to the microdistortions of the CeO_2 lattice were separated by applying the approximation method described by Gorelik et al. [36] to the peak pairs (200)/(400) and (111)/(222). The instrumental broadening was taken into account, which was determined from the diffraction pattern of the international standard corundum (α-Al_2O_3). The structure parameters of the CeO_2 phase (unit cell parameters; oxygen site occupancy; B factor, which characterizes the thermal and statistical displacements of atoms from their mean positions in the structure, i.e., structural disorder) and the quantitative phase composition of samples were determined by the full-profile analysis of diffraction patterns using the FullProf 2000 program package [37].

Catalytic Tests

CO oxidation in hydrogen-containing mixtures was carried out in a flow reactor at atmospheric pressure. The reactor was a U-shaped quartz tube with an inner diameter of 3 mm. The length of the catalyst bed was 40 mm. A 0.125-g portion of the catalyst was mixed with 0.2 g of quartz (particle diameter of 0.25–0.5 mm) and was placed in the reactor. The temperature was measured with a chromel–alumel thermocouple placed in the middle of the catalyst bed. The feed had the following composition (vol %): Co, 1; O_2, 1.5; H_2, 65; H_2O, 10; CO_2, 20; He, the balance. This is the composition that is most frequently used in the study of CO oxidation in hydrogen-containing mixtures. The flow rate of the gas mixture was 2 cm^3/s (STP). No catalyst pretreatment was applied before tests.

The concentrations of the reactants and products at the inlet and outlet of the reactor were measured on a Kristall-2000 chromatograph equipped with a methanator using the nickel catalyst NKM-4. The mixture to be analyzed was separated in a column packed with molecular sieve NaX (thermal conductivity detector) and a column packed with Porapak Q (flame-ionization detector). The sensitivity of the method made it possible to measure CO, CH_4, and CO_2 concentrations down to ~10^{-4} vol % and O_2 concentrations down to 10^{-3} vol %. In each test, the CO conversion (x_{CO}), O_2 conversion (x_{O_2}), and the selectivity of the reaction (S) were calculated using the equations

$$x_{CO} = \frac{[CO]_0 - [CO]}{[CO]_0} \times 100\%, \quad (1)$$

$$x_{O_2} = \frac{[O_2]_0 - [O_2]}{[O_2]_0} \times 100\%, \quad (2)$$

$$S = \frac{1}{2}\frac{[CO]_0 - [CO]}{[O_2]_0 - [O_2]} \times 100\%, \quad (3)$$

where $[CO]_0$ and $[O_2]_0$ are the inlet CO and O_2 concentrations and [CO] and $[O_2]$ are the corresponding outlet concentrations.

RESULTS AND DISCUSSION

Catalytic Activity

Catalytic tests were carried out at both increasing and decreasing temperatures. The temperature dependences of the CO and O_2 conversions and the selectivity of CO oxidation in the presence of hydrogen on the CeO_2 support and on the catalysts 1Cu-CeO_2, 5Cu-CeO_2, and 10Cu-CeO_2 are shown in Fig. 1. The same dependences obtained for the catalysts 10Cu-CeO_2, 15Cu-CeO_2, and 20Cu-CeO_2 are presented in Fig. 2. In all cases, x_{CO} first increases and then decreases with an increasing temperature. The maximum x_{CO} values are 58% at 420°C for CeO_2, 95% at 265°C for 1Cu-CeO_2, 99% at 210°C for 5Cu-CeO_2, 99% at 195°C for 10Cu-CeO_2, 98% at 185°C for 15Cu-CeO_2, and 96% at 200°C for 20Cu-CeO_2. The oxygen conversion increases with temperature and reaches 100% on CeO_2, 1Cu-CeO_2, 5Cu-CeO_2, 10Cu-CeO_2, 15Cu-CeO_2, and 20Cu-CeO_2 at 420, 270, 215, 195, 195, and 205°C, respectively.

The selectivity of the reaction on the copper-containing catalysts decreases gradually from ~90 to 60% and then, once the maximum CO and O_2 conversions are reached, decreases rapidly to 33%. As the temperature is further raised, both the CO conversion and the selectivity decrease. The selectivity of the reaction on CeO_2 is considerably lower than that on the copper–cerium oxide catalysts and gradually decreases from 45 to 20% as the temperature is raised.

The observed temperature dependences of x_{CO}, x_{O_2}, and S are fully reproduced in subsequent experiments performed at both decreasing and increasing temperatures. Thus, the catalytic properties of the samples remain unchanged in time.

As can be seen from the data presented in Figs. 1 and 2, the 15Cu-CeO_2 and 10Cu-CeO_2 systems are the most active. Below 185°C, x_{CO}, x_{O_2}, and S for these systems are nearly equal and are higher than the

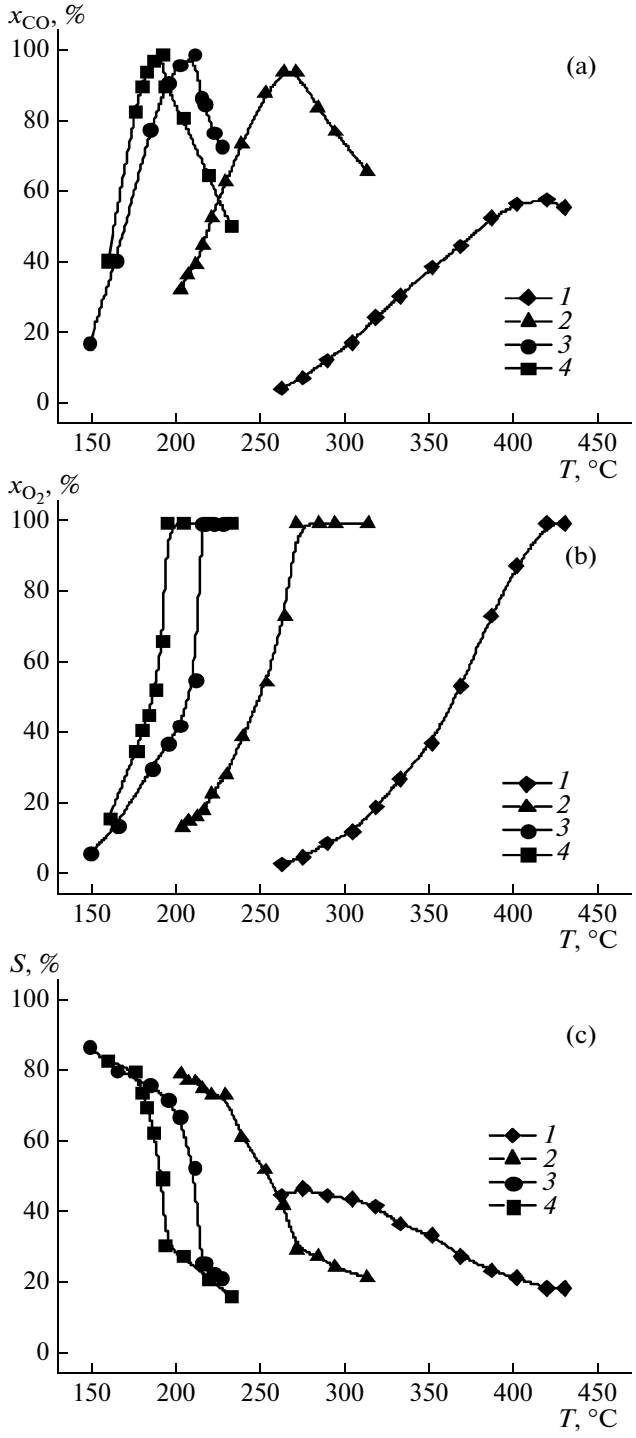

Fig. 1. Temperature dependences of the (a) CO conversion, (b) O_2 conversion, and (c) selectivity of CO oxidation in the presence of H_2 on the catalysts (*1*) CeO_2, (*2*) 1Cu-CeO_2, (*3*) 5Cu-CeO_2, and (*4*) 10Cu-CeO_2.

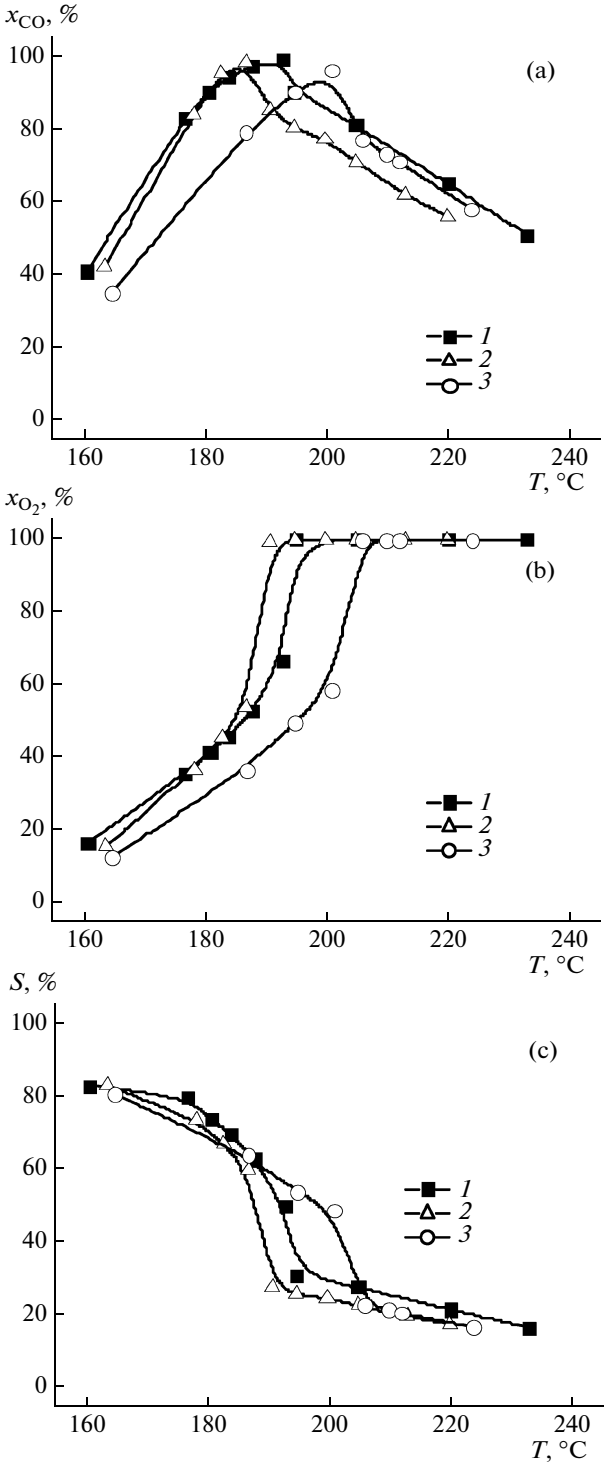

Fig. 2. Temperature dependences of the (a) CO conversion, (b) O_2 conversion, and (c) selectivity of CO oxidation in the presence of H_2 on the catalysts (*1*) 10Cu-CeO_2, (*2*) 15Cu-CeO_2, and (*3*) 20Cu-CeO_2.

same characteristics of the other systems. At higher temperatures, the 15Cu-CeO_2 catalyst is less selective than 10Cu-CeO_2 and, as a consequence, affords a smaller x_{CO} value at 100% O_2 conversion. The 5Cu-CeO_2 catalyst is somewhat less active than 15Cu-CeO_2, but is more selective, and, accordingly, the maximum CO conversion on this catalyst is higher.

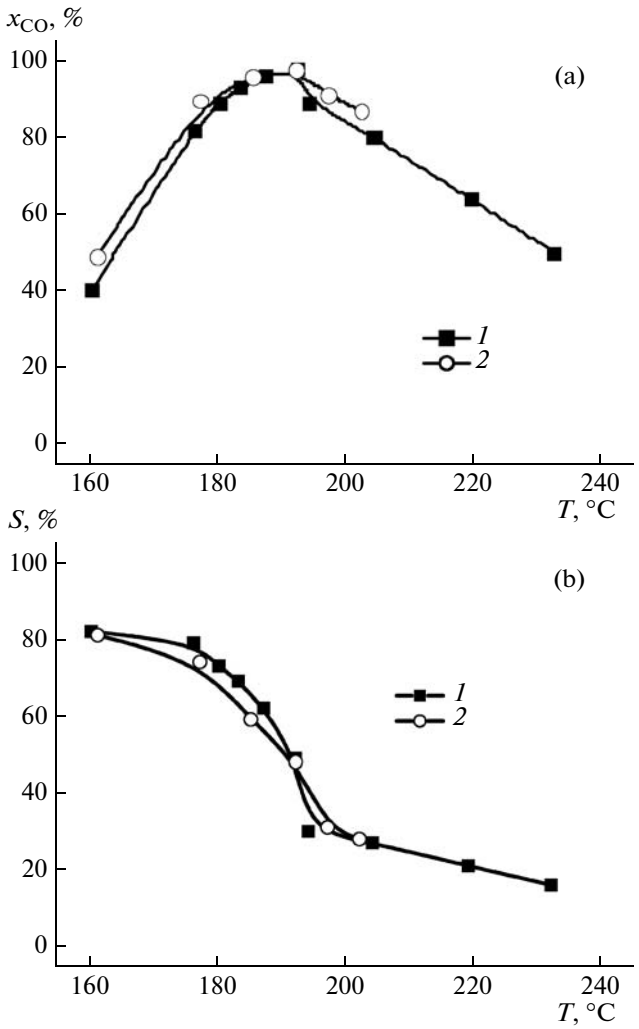

Fig. 3. Temperature dependences of the (a) CO conversion and (b) selectivity of CO oxidation in the presence of H_2 on the catalysts (*1*) 10Cu-CeO_2 and (*2*) 10 wt % Cu/CeO_2.

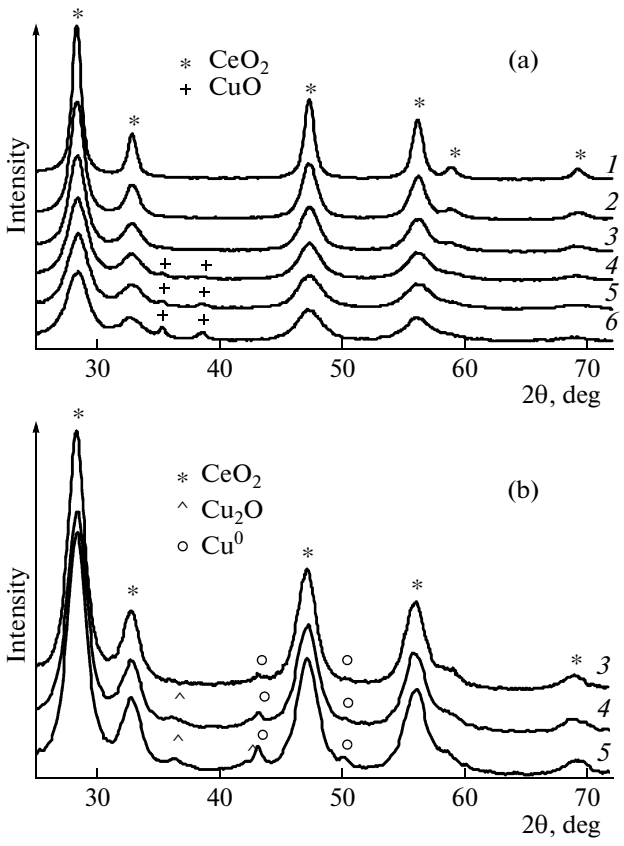

Fig. 4. Diffraction patterns of (*1*) CeO_2 and the catalysts (*2*) 1Cu-CeO_2, (*3*) 5Cu-CeO_2, (*4*) 10Cu-CeO_2, (*5*) 15Cu-CeO_2, and (*6*) 20Cu-CeO_2 (a) before and (b) after CO oxidation in hydrogen-containing mixtures on these samples.

Thus, the above results indicate that cerium dioxide is not inert and exhibits catalytic activity in CO oxidation in the presence of H_2. Even the introduction of small amounts of copper substantially enhances the activity and selectivity of this catalyst. An analysis of the activity and selectivity data demonstrates that 5Cu-CeO_2 and 10Cu-CeO_2 have optimum catalytic properties, ensuring the highest CO conversion. The 15Cu-CeO_2 catalyst, whose activity is similar to that of 10Cu-CeO_2, is inferior to this catalyst in selectivity. Similar results were obtained in our earlier studies for catalysts prepared by coprecipitation and impregnation [11, 12]. In Fig. 3, we compare the temperature dependences of the CO conversion and the selectivity of the reaction on the impregnated catalyst 10 wt % Cu/CeO_2 [11] and on the catalyst 10Cu-CeO_2 prepared by the Pechini method. Clearly, x_{CO} and S are similar for these catalysts. Thus, the catalyst prepared by the Pechini method is similar to the impregnated catalyst in catalytic properties.

Physicochemical Properties

The diffraction patterns of the CeO_2 support and 1Cu-CeO_2, 5Cu-CeO_2, 10Cu-CeO_2, 15Cu-CeO_2, and 20Cu-CeO_2 catalysts before the reaction are shown in Fig. 4a. The CuO phase is observed only in the catalysts containing more than 10 wt % copper. According to the results of quantitative phase analysis (table), only part of the copper in the catalysts containing 10–16.5 wt % Cu is in the form of the CuO phase ($D_{CuO} \approx 170$ Å). About 9 wt % copper in these samples is not detected by X-ray diffraction. This can be due to the small particle size of copper oxide in these materials or to the existence of a copper-containing phase resulting from the interaction between copper and cerium oxides.

The structure parameters of cerium dioxide determined by the full-profile analysis of diffraction patterns change as the copper content of the catalyst is increased. Firstly, the occupancy of oxygen sites in the structure decreases (the number of vacancies increases). This is likely due to the incorporation of

Properties of copper–cerium oxide catalysts

Sample	Copper content, wt %		S_{BET}, m^2/g	Structural and substructural parameters of CeO_2				Copper-containing phases**		
	chemical analysis	X-ray diffraction		D, Å	$\Delta d/d$	B^*_{Ce}, $Å^{-2}$	occupancy of oxygen sites	CuO	Cu	Cu_2O
CeO_2	0	–	27	115	0.001	0.0	1.00	–	–	–
1Cu-CeO_2 before reaction	0.95	–	66	75	0.002	0.22	1.00	–	–	–
5Cu-CeO_2 before reaction	4.85	–	69	60	0.003	0.30	0.98	–	–	–
5Cu-CeO_2 after reaction	–	~2.5	35	60	0.003	0.24	1.0	–	+	–
10Cu-CeO_2 before reaction	10.0	~1.2	76	50	0.004	0.43	0.94	+	–	–
10Cu-CeO_2 after reaction	–	5.8	42	50	0.003	0.39	1.0	–	+	+
15Cu-CeO_2 before reaction	13.6	3.2	61	50	0.004	0.46	0.93	+	–	–
15Cu-CeO_2 after reaction	–	7.8	22	50	0.002	0.39	0.98	–	+	+
20Cu-CeO_2 before reaction	16.5	7.2	55	45	0.004	0.62	0.90	+	–	–

Note: * B_{Ce} is the isotropic temperature factor of the cerium atoms. ** The signs + and – mean, respectively, the presence and absence of a given phase.

copper ions in a lower oxidation state into the CeO_2 structure. Secondly, the B factor increases, indicating progressive disordering of the CeO_2 lattice. The changes in these substructural characteristics of the support are evidence of increasing disordering: the CSR size of cerium oxide (D_{CeO_2}) decreases and the microdistortion of its lattice ($\Delta d/d$) increases as the copper content increases. Probably, this is due to the incorporation of an increasing number of copper ions into the CeO_2 lattice and to the formation of a solid solution. In addition, the catalyst particles form from an organic gel in which copper and cerium cations are distributed uniformly—a characteristic feature of the Pechini method. This is an obstacle to the formation of a well-crystallized cerium oxide phase.

For all of the starting samples, the unit cell parameter of the CeO_2 phase exceeds the standard value a = 5.411 Å (JCPDS file no. 34-0394) by 0.009 ± 0.001 Å. After the reaction, this parameter takes a larger value of 5.425 Å. This change in the unit cell parameter can be caused by the joint effect of the following factors: change in the composition, specifically, the incorporation of copper ions in different oxidation states, which have a smaller ionic radius, into the CeO_2 structure; change in defectivity, specifically, the formation of oxygen vacancies; and the size effect [38] (small size of crystallites). An analysis of these factors for each sample will be the subject of a special study. Here, we restrict ourselves to representation of experimental data.

On the whole, the above results are well consistent with the specific surface area data for the catalysts. As can be seen from the table, S_{BET} increases from 27 m^2/g for CeO_2 to 76 m^2/g for 10Cu-CeO_2 as the copper content is increased. In spite of the smaller CSR size of cerium oxide in 15Cu-CeO_2 and 20Cu-CeO_2, the smaller specific surface area of these samples is most likely due to the increase in the proportion of large copper oxide particles and the blocking of catalyst pores by these particles.

Figure 4b shows the diffraction patterns of the 5Cu-CeO_2, 10Cu-CeO_2, and 15Cu-CeO_2 catalysts that were exposed to the reaction medium. An analysis of the substructural and structural parameters of the CeO_2 phase in these catalysts (table) shows that, after the reaction, the number of oxygen vacancies and the disordering of the cerium oxide structure are lower, which is indicated by the decrease in the $\Delta d/d$ value and the B factor. These changes can likely be explained as follows: the reaction medium liberates part of the copper ions from the cerium dioxide structure, and these ions undergo reduction to form large particles of copper metal ($D \approx 160$ Å) and Cu_2O ($D \approx 60$ Å). Since the CSR size of cerium oxide remains unchanged during the reaction, the decrease in S_{BET} caused by the reaction is most likely due to the formation of a great number of large copper particles and blocking of support pores. Nevertheless, in spite of the extensive agglomeration of copper, part of the copper present in the catalysts (3–6 wt %) is not detected by X-ray diffraction after the reaction. This can be explained as follows. After the action of the reaction medium, this

part of copper remains in the cerium oxide structure or is a component of finely dispersed compounds strongly bound to the support surface. Since the catalysts 5Cu-CeO_2, 10Cu-CeO_2, and 15Cu-CeO_2 are similar in activity, we believe that it is the finely dispersed copper on the CeO_2 surface that is responsible for the oxidation of CO in the presence of H_2 (as in the case of the copper–cerium catalysts prepared by other methods). However, although the Pechini method affords finer initial copper particles in the catalyst than, for example, the coprecipitation or impregnation methods [11, 12], only part of the copper remains in the finely dispersed state after the action of the reaction medium, while the rest of it is agglomerated into large particles. Since the catalytic properties of the samples remain unchanged during the reaction and are reproduced in successive temperature increase–decrease cycles, it can be assumed that agglomeration under the action of the reaction medium occurs even at low temperatures. This assumption is based on experimental results obtained in an earlier study [12], in which the reduction of copper in copper–cerium catalysts prepared by coprecipitation and impregnation was shown by in situ IR spectroscopy to occur even at room temperature.

Thus, the reaction medium exerts a crucial effect on the final formation of the catalyst and its active sites, and, as a consequence, the catalytic properties of copper–cerium oxide catalysts prepared by other methods and containing the same amount of copper are similar.

ACKNOWLEDGMENTS

This work was supported in part by the BRHE program (grant no. Y4-C-08-12), Global Energy Foundation (grant no. MG-2007/04/1), and State contract no. 02.526.11.6006 in the framework of the Federal Central Project "Research and Development in the Priority Areas of the Development of the Science & Technology Complex of Russia in 2007–2012."

REFERENCES

1. Avgouropoulos, G., Ioannides, T., Matralis, H.K., Batista, J., and Hocevar, S., *Catal. Lett.*, 2001, vol. 73, p. 33.
2. Jung, C.R., Han, J., Nam, S.W., Lim, T.-H., Hong, S.-A., and Lee, H.-I., *Catal. Today*, 2004, vols. 93–95, p. 183.
3. Bae, Ch.M., Ko, J.B., and Kim, D.H., *Catal. Commun.*, 2005, vol. 6, no. 8, p. 507.
4. Liu, Zh., Zhou, R., and Zheng, X., *J. Mol. Catal. A: Chem.*, 2006, vol. 255, nos. 1–2, p. 103.
5. Zou, H., Dong, X., and Lin, W., *Appl. Surf. Sci.*, 2006, vol. 253, no. 5, p. 2893.
6. Pintar, A., Batista, J., and Hocevar, S., *J. Colloid Interface Sci.*, 2005, vol. 285, no. 1, p. 218.
7. Avgouropoulos, G., Ioannides, T., and Matralis, H., *Appl. Catal., B*, 2005, vol. 56, nos. 1–2, p. 87.
8. Liu, Zh., Zhou, R., and Zheng, X., *J. Mol. Catal. A: Chem.*, 2007, vol. 267, nos. 1–2, p. 137.
9. Kim, D.H. and Cha, J.E., *Catal. Lett.*, 2003, vol. 86, p. 107.
10. Avgouropoulos, G., Papavasiliou, J., Tabakova, T., Idakiev, V., and Ionnides, T., *Chem. Eng. J.*, 2006, vol. 124, nos. 1–3, p. 41.
11. Snytnikov, P.V., Stadnichenko, A.I., Semin, G.L., Belyaev, V.D., Boronin, A.I., and Sobyanin, V.A., *Kinet. Katal.*, 2007, vol. 48, no. 3, p. 463 [*Kinet. Catal.* (Engl. Transl.), vol. 48, no. 3, p. 439].
12. Snytnikov, P.V., Stadnichenko, A.I., Semin, G.L., Belyaev, V.D., Boronin, A.I., and Sobyanin, V.A., *Kinet. Katal.*, 2007, vol. 48, no. 3, p. 472 [*Kinet. Catal.* (Engl. Transl.), vol. 48, no. 3, p. 448].
13. Il'ichev, A.N., Firsova, A.A., and Korchak, V.N., *Kinet. Katal.*, 2006, vol. 47, no. 4, p. 602 [*Kinet. Catal.* (Engl. Transl.), vol. 47, no. 4, p. 585].
14. Martinez-Arias, A., Hungria, A.B., Munuera, G., and Gamarra, D., *Appl. Catal., B*, 2006, vol. 65, nos. 3–4, p. 207.
15. Gamarra, D., Hornes, A., Koppány, Zs., Schay, Z., Munuera, G., Soria, J., and Martínez-Arias, A., *J. Power Sources*, 2007, vol. 169, no. 1, p. 110.
16. Gamarra, D., Munuera, G., Hungria, A.B., Fernandez-Garcia, M., Conesa, J.C., Midgley, P.A., Wang, X.Q., Hanson, J.C., Rodriguez, J.A., and Martinez-Arias, A., *J. Phys. Chem. C*, 2007, vol. 111, no. 29, p. 11 026.
17. Gamarra, D., Belver, C., Fernandez-Garcia, M., and Martinez-Arias, A., *J. Am. Chem. Soc.*, 2007, vol. 129, no. 40, p. 12 064.
18. Sedmak, G., Hocevar, S., and Levec, J., *J. Catal.,* 2003, vol. 213, no. 2, p. 135.
19. Sedmak, G., Hocevar, S., and Levec, J., *J. Catal.,* 2004, vol. 222, no. 1, p. 87.
20. Avgouropoulos, G., Ionnides, T., Papadopolou, C., Batista, J., Hocevar, S., and Matralis, H.K., *Catal. Today,* 2002, vol. 75, nos. 1–4, p. 157.
21. Liu, Y., Fu, Q., and Stephanopoulos, M.F., *Catal. Today,* 2004, vols. 93–95, p. 241.
22. Avgouropoulos, G. and Ioannides, T., *Appl. Catal., A*, 2003, vol. 244, no. 1, p. 155.
23. Luo, M.-F., Ma, J.-M., Lu, J.-Q., Song, Y.P., and Wang, Y.-J., *J. Catal.,* 2007, vol. 246, no. 1, p. 52.
24. Marban, G. and Fuertes, A.B., *Appl. Catal., B*, 2005, vol. 57, no. 1, p. 43.
25. Avgouropoulos, G. and Ioannides, T., *Appl. Catal., B*, 2006, vol. 67, nos. 1–2, p. 1.
26. US Patent 3330697, 1967.
27. Gaki, A., Chrysafi, R., and Kakali, G., *J. Eur. Ceram. Soc.*, 2007, vol. 27, nos. 2–3, p. 1781.
28. Chiang, C., Shei, C.Y., Wu, S.F., and Huang, Y.T., *Appl. Phys. Lett.*, 1991, vol. 58, p. 2435.
29. Gulgun, M., Popoola, O.O., and Krieven, V.M., *J. Am. Ceram. Soc.*, 1994, vol. 77, p. 531.

30. Fernandes, J.D.G., Melo, D.M.A., Zinner, L.B., Salustiano, C.M., Silva, Z.R., Martinelli, A.E., Cerqueira, M., Alves Júnior, C., Longo, E., and Bernardi, M.I.B., *Mater. Lett.*, 2002, vol. 53, nos. 1–2, p. 122.
31. Guo, H., Yin, M., Dong, N., Xu, M., Lou, L., and Zhang, W., *Appl. Surf. Sci.*, 2005, vol. 243, nos. 1–4, p. 245.
32. Takamura, H., Enomoto, K., Kamegawa, A., and Okada, M., *Solid State Ionics*, 2002, vols. 154–155, p. 581.
33. Frolova-Borhert, Yu.V., Sadykov, V.A., Alikina, G.M., Lukashevich, A.I., Moroz, E.M., Kochubei, D.I., Kriventsov, V.V., Zaikovski, V.I., Zyryanov, V.V., and Uvarov, N.F., *Solid State Ionics*, 2006, vol. 177, nos. 26–32, p. 2533.
34. RF Patent Appl. 2008 131741, July 31, 2008.
35. JCPDS-JCDD Files, 1997.
36. Gorelik, S.S., Skakov, Yu. A., and Rastorguev, L.N., *Rentgenograficheskii i elektronno-opticheskii analiz* (X-Ray Diffraction and Electron Optical Analysis), Moscow: Mosk. Inst. Stali i Splavov, 1994, p. 130.
37. Rodriguez-Carvajal, J., *An Introduction to the Program Fullprof 2000, Version July 2001*, Gif-sur-Yvette, France: Laboratoire Leon Brillouin, 2001, p. 54.
38. Tsunekawa, S., Sivamohan, R., Ito, S., Kasuya, A., and Fukuda, T., *Nanostruct. Mater.*, 1999, vol. 11, p. 141.